L_p-NORM NON-NEGATIVE MATRIX FACTORIZATION AND ITS APPLICATION TO SINGING VOICE ENHANCEMENT

Tomohiko Nakamura[†] *and Hirokazu Kameoka*[†,‡]

[†]Graduate School of Information Science and Technology, The University of Tokyo.
7-3-1, Hongo, Bunkyo-ku, Tokyo, 113-8656, Japan.
[‡]NTT Communication Science Laboratories, Nippon Telegraph and Telephone Corporation.
3-1, Morinosato Wakamiya, Atsugi, Kanagawa, 243-0198, Japan
nakamura@hil.t.u-tokyo.ac.jp,kameoka@hil.t.u-tokyo.ac.jp

ABSTRACT

The measures of sparsity are useful in many audio signal processing such as speech enhancement, audio coding and singing voice enhancement, and the well-known method for these applications is non-negative matrix factorization (NMF), which decomposes a non-negative data matrix into two non-negative matrices. Although the previous studies of NMF have focused on the sparsity of the two matrices, the sparsity of reconstruction errors between a data matrix and the two matrices is also important, since designing the sparsity is equivalent to assuming the nature of the errors. Using the sparsity measure for NMF is difficult to solve the NMF because of the non-linearity of the sparsity measure. We propose a new NMF, which we called L_p-norm NMF, that minimizes the L_p norm of the reconstruction errors. We derive a computationally efficient algorithm of L_p-norm NMF, according to the auxiliary function principle. The algorithm has multiplicative update equations, and thus non-negativity of the model can be easily guaranteed. We further show that the algorithm of L_p-norm NMF can be generalized for factorizing the real-valued matrix into a product of two real-valued matrices. Throughout an experiment on singing voice enhancement, we confirm that the performance of the proposed algorithm using L_p-norm NMF was improved by adequately selecting p.

Index Terms— Non-negative matrix factorization, L_p norm, auxiliary function principle

1. INTRODUCTION

Non-negative matrix factorization (NMF) [1] is a powerful technique, which approximates a data matrix Y by a product of two non-negative matrices W and H. NMF has been actively studied in many scientific and engineering fields in recent years (see [2]), and particularly in the field of music signal processing, successful results were obtained by regarding a magnitude spectrogram as a non-negative matrix [3].

NMF is formulated as the minimization problem of a measure between a data matrix and the model. One standard measure is the Frobenius norm, and it corresponds to assuming that the reconstruction errors are additive Gaussian noise. While NMF with the Frobenius norm works well for the small errors, the performance of the NMF decreases for the large errors such as spike noise, even if there are a few elements of errors. We thus need to explore appropriate measures for the large errors.

As such measures, we can use the measures of sparsity such as the L_p norm, which with $p = 1$ is often employed instead of the L_0 norm in the field of sparse coding. Using the measures have been succeeded in many audio signal processing techniques such as NMF and robust principle component analysis [4, 5]. Many previous studies of NMF have used sparseness measures [6, 7], regularizers [8] and priors [9] on W, H, which induce sparse solutions. However, it is difficult to use the measures between a data matrix and the model directly, since the measures are frequenctly non-linear and solving the NMF is frequently intractable.

In this paper, we propose a new NMF, which we called L_p-norm NMF, that minimizes the L_p norm of reconstruction errors between a data matrix and the model. We formulate L_p-norm NMF with $0 < p \leq 2$ and derive a convergence-guaranteed algorithm that consists of multiplicative update equations for W and H based on the auxiliary function principle [10, 11]. The constant p controls the sparsity of the reconstruction errors, and the performance of L_p-norm NMF may be improved by adequately choosing p. To confirm the performance of L_p-norm NMF with different p, we apply L_p-norm NMF to singing voice enhancement for monaural audio signals.

We henceforth denote the set of real values and that of non-negative real values by $\mathbb{R}$ and $\mathbb{R}_{\geq 0}$.

2. L_p-NORM NON-NEGATIVE MATRIX FACTORIZATION

2.1. Problem setting

Let us define frequency, time, and basis indexes as $\omega \in [0, \Omega - 1]$, $t \in [0, T - 1]$ and $k \in [0, K - 1]$ such that $K < \min(\Omega, T)$. Given a non-negative data matrix $Y := \{y_{\omega,t}\}_{0\leq\omega\leq\Omega-1, 0\leq t\leq T-1}$, L_p-norm NMF is the problem of minimizing the L_p norm

$$\mathcal{L}(W, H) := \|Y - WH\|_p^p = \sum_{\omega,t} \left| y_{w,t} - \sum_k w_{\omega,k} h_{k,t} \right|^p \qquad (1)$$

subject to

$$\forall k, \ \sum_{\omega} W_{\omega,k} = 1. \qquad (2)$$

Here $W = \{w_{\omega,k}\}_{\omega,k}$ is a $\Omega \times K$ non-negative matrix and $H = \{h_{k,t}\}_{k,t}$ is a $K \times T$ non-negative matrix. Eq. (2) is introduced in order to avoid an indeterminacy in the scaling. When Y is a magnitude spectrogram, the columns of W represent spectral templates and the rows of H the temporal activities of the spectral templates.

The constant p controls the sparsity of the reconstruction error. Smaller p induces the sparsity, and most of the entries of the estimated data matrix WH are the same as those of Y, while the other entries were largely different from those of Y. On the other hand,

This work was supported by JSPS Grant-in-Aid for Young Scientists B Grant Number 26730100.

larger p does not induce the sparsity relatively, and all the entries of the estimated data matrix may be non-zero. We thus assume that the L_p norm satisfies $0 < p < 2$, which promotes sparsity. Note that when $p = 2$, the objective function equals to the NMF that minimizes the Euclidean distance of the reconstruction errors between a data matrix and the model.

2.2. Efficient algorithm based on auxiliary function principle

Since $\mathcal{L}(W, H)$ involves summation over k in the L_p norm, analytically solving the current minimization problem is intractable. However, we can develop a computationally efficient algorithm for finding a locally optimal solution based on the auxiliary function principle [10, 11].

When applying an auxiliary function principle to the minimization problem, the first step is to define an upper bound function for the objective function. Introducing auxiliary variables $\xi = \{\xi_{\omega,t} \in \mathbb{R}_{\geq 0}\}_{\omega,t}$, we derive

$$\Big|y_{w,t} - \sum_k w_{\omega,k}h_{k,t}\Big|^p \leq p\xi_{\omega,t}^{p-2}\Big|y_{w,t} - \sum_k w_{\omega,k}h_{k,t}\Big|^2 + (2-p)\xi_{\omega,t}^p. \quad (3)$$

The proof of the inequality is described in Lemma 2 of [12]. Equality of Eq. (3) holds if and only if

$$\xi_{\omega,t} = \Big|y_{\omega,t} - \sum_k w_{\omega,t}h_{k,t}\Big|. \quad (4)$$

The term in the square function of Eq. (3) includes summation over k, and we further derive the upper bound of the right-hand side of Eq. (3). Since the square function is a convex function, we can invoke the Jensen's inequality:

$$\Big(\sum_k w_{\omega,k}h_{k,t}\Big)^2 \leq \sum_k \frac{1}{\lambda_{\omega,t,k}}(w_{\omega,k}h_{k,t})^2 \quad (5)$$

where $\lambda = \{\lambda_{\omega,t,k} \in \mathbb{R}_{\geq 0}\}_{\omega,t,k}$ are auxiliary variables that sums to unity: $\sum_k \lambda_{\omega,t,k} = 1$. Equality of Eq. (5) holds if and only if

$$\lambda_{\omega,t,k} = \frac{w_{\omega,k}h_{k,t}}{\sum_{k'} w_{\omega,k'}h_{k',t}}. \quad (6)$$

The upper bound of $\mathcal{L}(W, H)$ can thus be described as

$$\begin{aligned}
&\mathcal{L}^+(W, H, \lambda, \xi) \\
&= \sum_{\omega,t} p\xi_{\omega,t}^{p-2}\Big\{y_{w,t}^2 - y_{\omega,t}\sum_k w_{\omega,k}h_{k,t} + \sum_k \frac{1}{\lambda_{\omega,t,k}}(w_{\omega,k}h_{k,t})^2\Big\} \\
&\quad + \sum_{\omega,t}(2-p)\xi_{\omega,t}^p. \quad (7)
\end{aligned}$$

We can derive update equations for the parameters, using the above upper bound. By setting at zero the partial derivative of $\mathcal{L}^+(W, H, \xi, \lambda)$ with respect to W and H and using Eq. (4) and Eq. (6), we obtain

$$W \leftarrow W \odot [\{(Y \oslash C)H^\top\} \oslash \{(WH \oslash C)H^\top\}] \quad (8)$$

$$H \leftarrow H \odot [\{W^\top(Y \oslash C)\} \oslash \{W^\top(WH \oslash C)\}] \quad (9)$$

where $\odot, \oslash$ denote element-wise product and division, and C is an $\Omega \times T$ matrix, whose (ω, t)-th element is

$$c_{\omega,t} = \Big|y_{\omega,t} - \sum_k w_{\omega,k}h_{k,t}\Big|^{2-p}. \quad (10)$$

It is worth noting that each update equation consists of multiplication by a non-negative factor. Hence, it is guaranteed that the entries of W and H are always non-negative when their initial values are set to non-negative values.

3. L_P-NORM MATRIX FACTORIZATION

3.1. Problem setting

While the algorithm is for non-negative matrices in the previous section, we can generalize the algorithm for real-valued matrices, according to the auxiliary function principle. We call the problem L_p-norm matrix factorization (L_p-norm MF).

L_p-norm MF is the problem of finding real-valued matrices W, H for a given real-valued data matrix Y such that

$$\min_{W\in\mathbb{R}^{\Omega\times K}, H\in\mathbb{R}^{K\times T}} \mathcal{J}(W, H) = \|Y - WH\|_p^p,$$
$$\text{subject to } \forall k, \ \sum_\omega W_{\omega,k} = 1$$

where $0 < p < 2$ and $\mathcal{J}(W, H)$ is the objective function.

3.2. Iterative algorithm based on auxiliary function principle

As similar as Sec. 2, $\mathcal{J}(W, H)$ involves summation over k in the L_p norm, and we consider the upper bound of $\mathcal{J}(W, H)$ to apply the auxiliary function principle to the intractable minimization problem. The inequality used in Eq. (3) is applicable to $\mathcal{J}(W, H)$, and the upper bound of $\mathcal{J}(W, H)$ is the same as the right-hand side of Eq. (3). To derive the upper bound of the square function of Eq. (3), we can use the generalization of the Jensen's inequality for $y_{\omega,t}, w_{\omega,k}, h_{k,t} \in \mathbb{R}$, which was employed in [12]:

$$\Big|y_{\omega,t} - \sum_k w_{\omega,k}h_{k,t}\Big|^2 \leq \sum_k \frac{|\alpha_{\omega,t,k} - w_{\omega,k}h_{k,t}|^2}{\beta_{\omega,t,k}} \quad (11)$$

where $\alpha = \{\alpha_{\omega,t,k} \in \mathbb{R}\}_{\omega,t,k}, \beta = \{\beta_{\omega,t,k} \in [0, 1]\}_{\omega,t,k}$ are auxiliary variables subject to $\sum_k \alpha_{\omega,t,k} = y_{\omega,t}, \sum_k \beta_{\omega,t,k} = 1$. Equality of Eq. (11) holds if and only if

$$\alpha_{\omega,t,k} = w_{\omega,k}h_{k,t} - \beta_{\omega,t,k}\Big(\sum_{k'} w_{\omega,k'}h_{k',t} - y_{\omega,t}\Big). \quad (12)$$

The upper bound of $\mathcal{J}^+(W, H)$ can thus be described as

$$\mathcal{J}^+(W, H, \xi, \alpha, \beta) = \sum_{\omega,t} p\xi_{\omega,t}^{p-2}\sum_k \frac{|\alpha_{\omega,t,k} - w_{\omega,k}h_{k,t}|^2}{\beta_{\omega,t,k}} + (2-p)\xi_{\omega,t}^p. \quad (13)$$

By differentiating $\mathcal{J}^+(W, H, \xi, \alpha, \beta)$ partially with respect to W and H and setting them at zero, we can obtain the update equations:

$$w_{\omega,k} \leftarrow \frac{\sum_t c_{\omega,t}^{-1}h_{k,t}\Big(\beta_{\omega,t,k}^{-1}w_{\omega,k}h_{k,t} + y_{\omega,t} - \sum_{k'} w_{\omega,k'}h_{k',t}\Big)}{\sum_t c_{\omega,t}^{-1}\beta_{\omega,t,k}^{-1}h_{k,t}^2} \quad (14)$$

$$h_{k,t} \leftarrow \frac{\sum_\omega c_{\omega,t}^{-1}w_{\omega,k}\Big(\beta_{\omega,t,k}^{-1}w_{\omega,k}h_{k,t} + y_{\omega,t} - \sum_{k'} w_{\omega,k'}h_{k',t}\Big)}{\sum_\omega c_{\omega,t}^{-1}\beta_{\omega,t,k}^{-1}w_{\omega,k}^2} \quad (15)$$

where $c_{\omega,t}$ is defined as Eq. (10).

3.3. Relation to L_p-norm NMF

The parameters β can be chosen arbitrarily subject to $\beta_{\omega,t,k} \in \mathbb{R}_{\geq 0}$ and $\sum_k \beta_{\omega,k,t} = 1$. Choosing β as in [12], we obtain the multiplicative update equations as same as Eq. (8) and Eq. (9). Therefore, we can say that the algorithm of L_p NMF is the special case of that of L_p MF.

4. APPLICATION TO SINGING VOICE ENHANCEMENT

4.1. Singing voice enhancement

In this section, we apply L_p-norm NMF to singing voice enhancement for monaural audio signals, which enhances a singing voice signal from a monaural mixed audio signal consisting of vocal and accompaniment parts. Singing voice enhancement is often used in music information retrieval (MIR) applications such as automatic lyrics recognition [13, 14], automatic singer identification [15], and automatic karaoke generator [16].

When input audio signals are multichannel, we can use spatial cues, following the fact that vocal parts of music audio signals are frequently mixed at the center of the sound field. However, for monaural inputs, we need other cues instead of the spatial cues.

4.2. Enhancement algorithm

We utilize a fact on difference between accompaniment spectrograms and singing voice spectrograms. Accompaniment sounds are generated by musical instruments, and they reproduce the approximately same sounds each time when they are played. We can see the spectrograms of accompaniment signals as a low-rank matrix. On the contrary, singers fluctuate their singing voice for musical expressions such as vibrato, and singing voices typically have fluctuations (relatively, high rank) in the time-frequency domain, while it is known that the spectrograms of singing voices are sparse. We can thus enhance the singing voice component of a input spectrogram, by decreasing the low-rank component of the spectrogram with sparsity constraints on the rest component.

As mentioned in Sec. 2.1, the model spectrogram WH of L_p-norm NMF is a non-negative matrix with the rank of K, and small p induces the sparsity of the reconstruction errors. Setting K and p to small enough, we expect the low-rank matrix WH to contain accompaniment signals and the reconstruction errors $Y - WH$ to contain singing voice signals.

Let the estimated magnitude spectrogram of singing voice be $\hat{S} = \{\hat{s}_{\omega,t}\}_{0\leq\omega\leq\Omega-1, 0\leq t\leq T-1}$. First, an input signal including singing voice and accompaniment is converted into the complex spectrogram by short-time Fourier transform (STFT). We interpret the magnitude spectrogram of the input signal as a non-negative matrix, and apply L_p-norm NMF to the magnitude spectrogram. The obtained model spectrogram WH should correspond to the accompaniment, and the reconstruction errors between the observed magnitude spectrogram and the model spectrogram corresponds to the singing voice. The time-frequency components of the model spectrogram may be larger than those of the observed spectrogram, and we derive $\hat{S}$ as

$$\hat{s}_{\omega,t} = \begin{cases} y_{\omega,t} - \sum_k w_{\omega,k}h_{k,t} & (y_{\omega,t} \geq \sum_k w_{\omega,k}h_{k,t}) \\ 0 & (y_{\omega,t} < \sum_k w_{\omega,k}h_{k,t}) \end{cases}. \quad (16)$$

The estimated magnitude spectrogram with the phase of the original complex spectrogram is converted into an audio signal by the inverse STFT.

5. EXPERIMENTAL EVALUATION

5.1. Experimental conditions

To evaluate the performance of the proposed method, we conducted two experiments on the singing voice enhancement: an evaluation of the effect of p, which controls sparsity, and frame length F, and a comparison of our results with the state-of-the-arts [5, 17, 18].

The criteria for the performance evaluation of singing voice enhancement were the normalized signal-to-distortion ratio (NSDR) and the global NSDR (GNSDR), which were defined as

$$\mathrm{NSDR}(\{\hat{f}_t\}_t; \{f_t\}_t, \{x_t\}_t) = \mathrm{SDR}(\{\hat{f}_t\}_t, \{f_t\}_t) - \mathrm{SDR}(\{x_t\}_t, \{f_t\}_t), \quad (17)$$

$$\mathrm{GNSDR} = \frac{\sum_i w_i \mathrm{NSDR}(\{\hat{f}_{i,t}\}_t; \{f_{i,t}\}_t, \{x_{i,t}\}_t)}{\sum_i w_i}, \quad (18)$$

$$\mathrm{SDR}(\{\hat{f}_t\}_t, \{f_t\}_t) = 10 \log_{10} \frac{\sum_t \hat{f}_t f_t}{\left(\sum_t \hat{f}_t\right)\left(\sum_t f_t\right) - \sum_t \hat{f}_t f_t}, \quad (19)$$

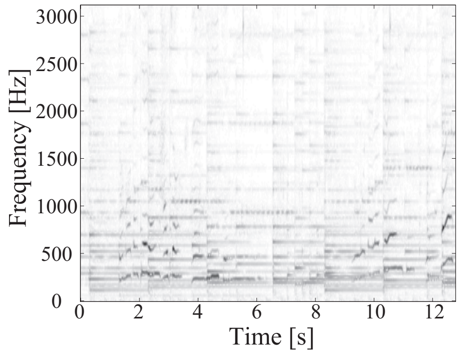

(a) Spectrogram of input audio signal.

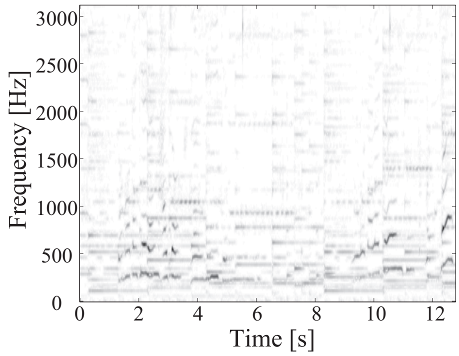

(b) Spectrogram of audio signal after enhancement.

Fig. 1. Spectrogram examples of (a) a mixed audio signal and (b) the singing-voice-enhanced audio signal by the proposed method.

where $\hat{f}_{i,t}$, $f_{i,t}$ and $x_{i,t}$ denote the estimated signal, the target signal and the input signal of the i-th piece. NSDR represents the improvement of SDR, and GNSDR denotes the weighted averages of NSDR of all music pieces by the length of the i-th piece, $\{w_i\}_i$. These criteria were also employed in many previous works [5, 17–20]. For the calculation of SDR, we used the BSS Eval Toolbox [21, 22].

As an evaluation dataset, we used the MIR-1K dataset [23], following the evaluation framework in [5, 17, 18]. The dataset consists of 1000 Chinese song clips by amateur singers. The durations of the clips ranges from 4 to 13 s, and the audio signals were monaural with a sampling rate of 16 kHz. The accompaniment and vocal parts were recorded separately, and we could mix them in any signal-to-noise ratio (SNR), where the SNR corresponds to voice to accompaniment ratio. The accompaniment and vocal parts for each clip were mixed at −5 dB (accompaniment is louder), 0 dB (same level) and 5 dB (vocal is louder) SNRs.

5.2. Effect of sparsity and frame lengths

We first compared the proposed method in p and F. We used $p = 0.1, 0.2, \cdots, 2.0$ and $F = 512, 1024, 2048, 4096$ sample points. For STFT, a window function was the sin window, and the frame shifts were half the length of the frames. The number of bases was set at $K = 10$. The entries of W and H were initialized randomly. The number of iterations were 200, which is supposed to be sufficient empirically.

Fig. 1 shows one of the enhanced results with the proposed method. The figures illustrate the spectrograms of an input signal and the enhanced result. We can see that most of accompanying sounds (vertically and horizontally smooth component) are suppressed, and the singing voice component of the spectrogram is clearer than that of the input spectrogram.

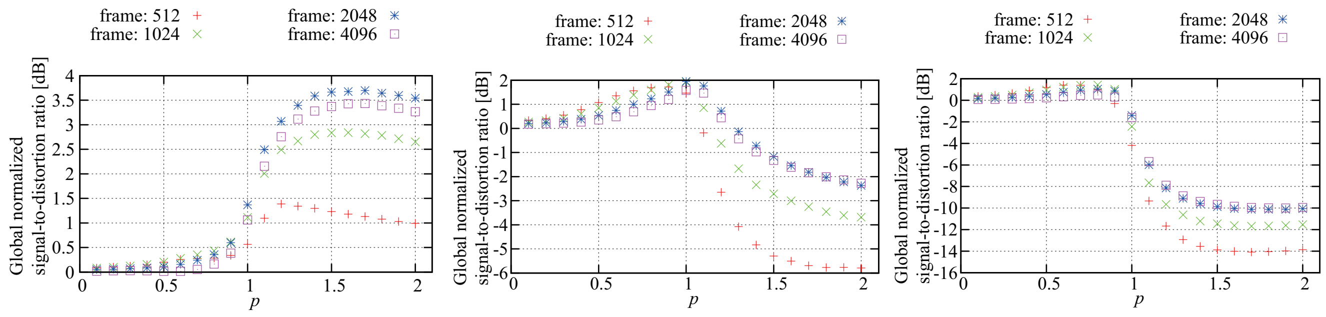

(a) GNSDR at −5 dB SNR. (b) GNSDR at 0 dB SNR. (c) GNSDR at 5 dB SNR.

Fig. 2. Global normalized signal-to-distortion ratio (GNSDR) of the proposed method with respect to p of the L_p norm and frame length F. Red, blue, green and purple points correspond to $F = 512, 1024, 2048, 4096$ sample points. The results are for (a) −5 dB, (b) 0 dB, and (c) 5 dB SNRs.

Table 1. Global normalized signal-to-distortion ratio (GNSDR) comparison with previous works. F denotes the length of a frame in sample point. Hsu, Rafii and Huang represent corresponding methods [5, 17, 18].

Input SNR [dB]	Proposed method $F = 1024$	Proposed method $F = 2048$	Hsu [17]	Rafii [18]	Huang [5]
−5	2.84 ($p = 1.6$)	3.70 ($p = 1.7$)	−0.51	0.52	1.51
0	1.93 ($p = 1.0$)	1.95 ($p = 1.0$)	0.91	1.11	2.37
5	1.43 ($p = 0.8$)	1.04 ($p = 0.8$)	0.17	1.10	2.57

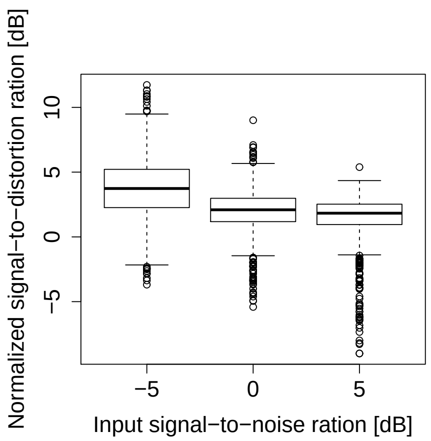

Fig. 3. Box plot of normalized signal-to-distortion ratio (NSDR) of the proposed method for MIR-1K dataset. The results for −5, 0, 5 dB SNRs are for $(p, F) = (1.7, 2048), (1.0, 2048), (0.8, 1024)$, respectively.

As illustrated in Fig. 2 for −5, 0, 5 dB SNRs, the results show that the GNSDRs highly depended on p with all frame lengths. The highest GNSDRs for all SNRs were 3.7 at $(p, F) = (1.7, 2048)$ for −5 dB SNR, 1.95 at $(p, F) = (1.0, 2048)$ for 0 dB SNR, and 1.43 at $(p, F) = (0.8, 1024)$ for 5 dB SNR. We can see that p at which GNSDR were highest for each input SNR decreased as input SNR became higher. With high input SNR, the non-zero time-frequency components of the singing voice spectrogram are large, and increasing the sparsity is preferred. On the other hand, with low input SNR, the non-zero time-frequency components are small, and decreasing the sparsity is preferred. The obtained results are consitent with the consideration.

Fig. 3 illustrates the distributions of NSDRs for each SNR. The results were for $(p, F) = (1.7, 2048), (1.0, 2048), (0.8, 1024)$ for −5, 0, 5 dB SNRs. Since most of NSDRs were larger than 0 dB, and we can confirm that the proposed method worked well for most of the input signals.

5.3. Comparison with previous works

We finally compared the proposed method with the state-of-the-arts [5, 17, 18]. The results were described in Tab. 1. The proposed method with $F = 1024$ outperformed two previous methods for all input SNRs. While the GNSDRs of the proposed method were lower than those of [5] in 0, 5 dB SNRs, the GNSDR of the proposed method is 0.4 to 2.4 dB larger than those of three previous methods significantly at −5 dB SNR. This result indicates that the proposed method works well particularly in the low SNR environment.

6. CONCLUSION

We proposed a new NMF that minimizes the L_p norm of the reconstruction errors between a data matrix and the model. According to the auxiliary function principle, the computationally efficient algorithm was derived, and it has multiplicative update equations, which guarantee the non-negativity of W and H. The algorithm of L_p-norm NMF can be generalized for that of L_p-norm MF for real-valued matrices. We apply L_p-norm NMF to singing voice enhancement. The experiments on singing voice enhancement showed that the performance of the proposed method could be improved by selecting p adequately, and the proposed method outperformed three previous works for low SNR condition.

There are several ways to extend L_p-norm NMF to other applications. One promising application is speech enhancement, since the spectrogram of background noise is sometimes approximated to be low rank and the speech spectrogram is relatively sparse.

7. REFERENCES

[1] D. D. Lee and H. S. Seung, "Learning the parts of objects by non-negative matrix factorization," *Nature*, vol. 401, no. 6755, pp. 788–791, 1999.

[2] Y.-X. Wang and Y.-J. Zhang, "Nonnegative matrix factorization: A comprehensive review," *IEEE Trans. Knowl. Data Eng.*, vol. 25, no. 6, pp. 1336–1353, 2013.

[3] P. Smaragdis and J. C. Brown, "Non-negative matrix factorization for polyphonic music transcription," in *Proc. IEEE Workshop Applications Signal Process. Audio Acoust.* IEEE, 2003, pp. 177–180.

[4] J. Wright, A. Ganesh, S. Rao, Y. Peng, and Y. Ma, "Robust principal component analysis: Exact recovery of corrupted low-rank matrices via convex optimization," in *Proc. Adv. Neural Inf. Process. Syst.*, 2009, pp. 2080–2088.

[5] P.-S. Huang, S. D. Chen, P. Smaragdis, and M. Hasegawa-Johnson, "Singing-voice separation from monaural recordings using robust principal component analysis," in *Proc. Int. Conf. Acoust. Speech Signal Process.*, 2012, pp. 57–60.

[6] P. O. Hoyer, "Non-negative sparse coding," in *IEEE Workshop Neural Networks for Signal Process.*, 2002, pp. 557–565.

[7] P. O. Hoyer, "Non-negative matrix factorization with sparseness constraints," *J. Mach. Learn. Res.*, vol. 5, pp. 1457–1469, 2004.

[8] B. Shen, L. Si, R. Ji, and B.-D. Liu, "Robust nonnegative matrix factorization via l_1 norm regularization," *CoRR*, vol. abs/1204.2311, 2012.

[9] T. Virtanen, A. T. Cemgil, and S. Godsill, "Bayesian extensions to non-negative matrix factorisation for audio signal modelling," in *Proc. Int. Conf. Acoust. Speech Signal Process.*, Mar. 2008, pp. 1825–1828.

[10] J. M. Ortega and W. C. Rheinboldt, *Iterative solution of nonlinear equations in several variables*, Number 30. 2000.

[11] H. Kameoka, M. Goto, and S. Sagayama, "Selective amplifier of periodic and non-periodic components in concurrent audio signals with spectral control envelops," in *Proc. SIG Tech. Reports on Music and Computer of IPSJ*, Aug. 2006, vol. 2006-MUS-66, pp. 77–84, in Japanese.

[12] H. Kameoka, N. Ono, K. Kashino, and S. Sagayama, "Complex NMF: A new sparse representation for acoustic signals," in *Proc. Int. Conf. Acoust. Speech Signal Process.*, 2009, pp. 3437–3440.

[13] M. Suzuki, T. Hosoya, A. Ito, and S. Makino, "Music information retrieval from a singing voice using lyrics and melody information," *EURASIP J. Applied Signal Process.*, vol. 2007, no. 1, pp. 151–151, 2007.

[14] A. Mesaros and T. Virtanen, "Automatic recognition of lyrics in singing," *EURASIP J. Audio, Speech, and Music Process.*, vol. 2010, no. 4, pp. 1–7, 2010.

[15] H. Fujihara, T. Kitahara, M. Goto, K. Komatani, T. Ogata, and H. G. Okuno, "Singer identification based on accompaniment sound reduction and reliable frame selection," in *Proc. Int. Symposium Music Info. Retrieval*, 2005, pp. 329–336.

[16] M. Ryynänen, M. Virtanen, J. Paulus, and A. Klapuri, "Accompaniment separation and karaoke application based on automatic melody transcription," in *Proc. IEEE Int. Conf. Multimedia Expo*, 2008, pp. 1417–1420.

[17] C.-L. Hsu and J.-S. R. Jang, "On the improvement of singing voice separation for monaural recordings using the mir-1k dataset," *IEEE Trans. Acoust., Speech, and Language Process.*, vol. 18, no. 2, pp. 310–319, 2010.

[18] Z. Rafii and B. Pardo, "A simple music/voice separation method based on the extraction of the repeating musical structure," in *Proc. Int. Conf. Acoust. Speech Signal Process.*, 2011, pp. 221–224.

[19] A. Ozerov, P. Philippe, R. Gribonval, and F. Bimbot, "One microphone singing voice separation using source-adapted models," in *Proc. IEEE Workshop Applications Signal Process. Audio Acoust.*, 2005, pp. 90–93.

[20] H. Tachibana, N. Ono, and S. Sagayama, "Singing voice enhancement in monaural music signals based on two-stage harmonic/percussive sound separation on multiple resolution spectrograms," *IEEE/ACM Trans. Audio, Speech and Language Process.*, vol. 22, no. 1, pp. 228–237, 2014.

[21] E. Vincent, R. Gribonval, and C. Févotte, "Performance measurement in blind audio source separation," *IEEE Trans. Acoust., Speech, and Language Process.*, vol. 14, no. 4, pp. 1462–1469, 2006.

[22] "Bss eval," `http://bass-db.gforge.inria.fr/bss_eval/`.

[23] "Mir-1k dataset," `https://sites.google.com/site/unvoicedsoundseparation/mir-1k`.